

# Atmospheric concentration, temporal and spatial variations, and sources identification of persistent organic pollutants in urban and semi-urban areas using the passive air samplers

Mehmet Ferhat Sari

Bursa Uludag Universitesi

Fatma Esen (✉ [payan@uludag.edu.tr](mailto:payan@uludag.edu.tr))

Bursa Uludag Universitesi <https://orcid.org/0000-0002-1445-0868>

---

## Research Article

**Keywords:** Passive air samplers, PAHs, PCBs, OCPs, Temporal variation

**Posted Date:** July 8th, 2021

**DOI:** <https://doi.org/10.21203/rs.3.rs-674900/v1>

**License:** © ⓘ This work is licensed under a Creative Commons Attribution 4.0 International License.

[Read Full License](#)

---

# Abstract

In this study, the ambient persistent organic pollutants (POPs) such as polycyclic aromatic hydrocarbons (PAHs), polychlorinated biphenyls (PCBs), and organochlorine pesticides (OCPs) concentrations were measured for 12 months at urban and semi-urban areas using the passive air sampler. During the sampling period, a total of 14 PAH ( $\sum_{14}\text{PAH}$ ) concentrations measured in urban and semi-urban areas were found as  $54.4 \pm 22.6 \text{ ng/m}^3$  and  $51.7 \pm 34.3 \text{ ng/m}^3$ , respectively. Molecular diagnostic ratios (MDRs) were used to determine PAH sources. According to the MDR values, combustion sources are the most important PAH sources in both sampling areas. However, since the urban area is close to the industrial zone, the combustion sources occurred at high temperatures ( $> 800 \text{ }^\circ\text{C}$ ), while the semi-urban area generally consisted of burning petrogenic fuels.  $\sum_{50}\text{PCB}$  concentrations measured in the urban and semi-urban areas were found as  $522.5 \pm 196.9 \text{ pg/m}^3$  and  $439.5 \pm 166.6 \text{ pg/m}^3$ , respectively. Homologous group distributions were used to determine the source of PCBs. According to homologous group distributions, Tri-, Tetra-, and Penta- chlorinated PCBs were dominant in both sampling areas.  $\sum_{10}\text{OCP}$  concentrations measured in urban and semi-urban areas were found as  $242.5 \pm 104.6 \text{ pg/m}^3$  and  $275.9 \pm 130.9 \text{ pg/m}^3$ , respectively. Also,  $\alpha\text{-HCH}/\gamma\text{-HCH}$  and  $\beta/(\alpha + \gamma)\text{-HCH}$  ratios were used to determine the source of OCPs. Lindane was the predominated OCP in both sampling areas.

## 1. Introduction

Persistent organic pollutants (POPs) are chemicals that have biological accumulation, persistence, toxicities, carcinogenic effects, a large number of natural and anthropogenic sources and have been widely used since the Second World War (Estellano et al. 2017; Ontiveros-Cuadras et al. 2019). These compounds can also be transported over long distances in the atmosphere (Wang et al. 2020b). The Stockholm Convention was signed in 2001 to reduce the environmental levels and emissions of POPs (Ruggeri et al. 2020).

Polycyclic aromatic hydrocarbons (PAHs), polychlorinated biphenyls (PCBs) and organochlorine pesticides (OCPs) are the well-known POPs (Qu et al. 2019). PAHs are contaminants formed by combining two or more benzene rings that are clustered, angularly, or linearly connected (Naing et al. 2020). PAHs have stable molecular structures since they come together with  $\pi - \pi$  bonds (Zhang et al. 2020a). There are both anthropogenic and natural sources of PAHs. Anthropogenic sources are usually caused by the incomplete combustion of coal, wood, oil, organic compounds (Naing et al. 2020). Natural sources of PAHs include volcanic eruptions and the open burning of fossil fuels (Gaurav et al. 2021). Although PCBs have historically been widely used in dielectric fluids and transformers, they were banned in the 1970s due to their high bioaccumulation and toxicity properties (Wang et al. 2011). OCPs were first used frequently as synthetic insecticides between the 1940s and 1960s. However, it was banned worldwide in the 1980s due to its negative characteristics for the environment and human health (Chen et al. 2020a).

Molecular diagnostic ratios (MDRs) are used as a qualitative method to investigate the transport and fate of PAHs in a specific environment (Zhang et al. 2020b). This source identification method plays an essential role in determining emission sources. Volatile and semi-volatile PAH compounds vary widely at greater distances from the source region due to different reaction rates (Ji et al. 2019). Most MDRs consist of PAH pairs with the same molecular mass and physicochemical properties (Amador-Muñoz et al. 2020). Homolog group distributions of PCBs are generally used to determine the distribution, transportation, and fate of PCB resources in the environment (Habibullah-Al-Mamun et al. 2019). Since the low chlorinated PCBs have higher vapor pressures, they can be moved further away from a source (Hu et al. 2019). Therefore, the determination of homolog group distributions is critical in the source identification of PCBs. Diagnostic ratios are widely used to identify the sources of OCPs.  $\alpha$ -HCH/ $\gamma$ -HCH and  $\beta$ /( $\alpha + \gamma$ )-HCH ratios are often used to identify possible sources (Kong et al. 2014; Sah et al. 2020).

The majority of researchers focused on pollutant concentrations and their distribution between sampling points. In this study, the concentrations of different pollutants, their distribution between the sampling points and their sources, as well as their temporal and spatial changes were investigated. The specific objectives of the present study were to; i) measure the concentrations of PAHs, PCBs and OCPs in the urban and semi-urban areas, ii) identify the possible sources, and iii) the determination of temporal and regional changes of concentration values.

## 2. Material And Methods

### 2.1. Sampling areas, program and preparation

Bursa is Turkey's 4th largest city in terms of population, with about 3 million inhabitants. Also, Bursa, according to industry statistics inventory, is Turkey's largest industrial and automotive manufacturing center. Therefore, traffic, industry, and domestic heating are among the primary sources of air pollution in Bursa. Also, air pollution is felt more with the topographic structure of Bursa and the decrease of existing winds, especially in winter. In this study, ambient air samples were taken from urban and semi-urban areas in Bursa (Turkey) using a passive air sampler (PAS). The urban sampling area (40° 17'11.16" N – 29° 5'13.20 "E) is approximately 1.5 km from the Bursa-Ankara highway, 3 km from the industrial zone and 500 m from the nearest settlement. The semi-urban sampling area (40° 10'8.30 "N – 29° 10'26.82 "E) is approximately 2 km from the nearest highway and 3 km from the nearest settlement.

Air samples were collected monthly between May 2017 and April 2018 using PASs. The PASs were placed on a branch of a tree 1–2 meters in height in the urban sampling area and on a platform 2 meters above the ground in the semi-urban sampling area. Sampling rates ( $R_s$ ) values for individual POP compounds targeted in this study were calculated according to the model proposed by Herkert et al. (2016) ([http://s-iihr41.iihr.uiowa.edu/pufpas\\_model](http://s-iihr41.iihr.uiowa.edu/pufpas_model)). Since the  $R_s$  values were calculated for each POP compound and each sampling site, atmospheric POP concentrations were determined successfully. In this context, the calculated  $R_s$  values were given in Table S1 (Supplementary material).

## 2.2. Sampling and Instrumental Analysis

The PUF disks were cleaned before being taken to the sampling area. First, the cleaning procedure was carried out with soxhlet extraction using purified water, then acetone (ACE) (Merck, Darmstadt, Germany) (two times), and finally hexane (HEX) (Merck, Darmstadt, Germany). Each processing step lasted 24 hours. After the cleaning process, the PUF discs were dried using a vacuum desiccator. Next, it was wrapped in aluminum foils until taken to the sampling area and kept in a deep freezer at -20 °C.

The PUF discs after sampling were extracted with the 300 mL ACE/HEX (v/v, 1/1) mixture for 24 hours using the soxhlet extraction method (Esen 2013; Sari et al. 2020a). In order to determine analytical efficiency, 1 mL of surrogate solution was added to samples before extraction. Extracted PUF discs were concentrated by rotary evaporator (Laborota 4001 Model, Heidolph, Germany). The rotary evaporator was operated for 30 rpm and 22–23 °C. Sample volumes were first reduced to 5 mL, then 10 mL of HEX was added and finally reduced to 2 mL (Tasdemir et al. 2012; Sari et al. 2020a). The purpose of using a rotary evaporator is to exchange the solvent for hexane.

The samples exchanged to hexane were fractionated using a fractioning column consisting of glass fiber wool, 3 grams of silicic acid hydrate (Sigma-Aldrich, 60780), 2 grams of aluminium oxide (Merck, Darmstadt, Germany) and 2 grams of sodium sulfate ( $\text{Na}_2\text{SO}_4$ ) (Merck, Darmstadt, Germany). The fraction column was cleaned using 20 mL of dichloromethane (DCM) (Merck, Darmstadt, Germany) and 20 mL of petroleum ether (PE) (Merck, Darmstadt, Germany) to prevent possible contamination in the environment. Subsequently, 2 mL volumes of samples were passed through the column. 25 mL PE was used for the elution of target PCBs (fraction 1), and 20 mL DCM was used for the elution of target PAHs and OCPs (fraction 2) (Cindoruk 2011; Esen 2013; Sari et al. 2020a). Finally, the sample volume was reduced again to 1 mL with the rotary evaporator. PCBs samples were cleaned with high purity sulfuric acid ( $\text{H}_2\text{SO}_4$ ) (97–99%) for possible contamination (Günindi and Tasdemir 2010; Tasdemir et al. 2012).

Analysis of PCB and OCPs were determined using the gas chromatograph (GC) device with the Agilent 7890A model micro-electron capture detector ( $\mu\text{ECD}$ ). Similarly, PAH analysis was performed using Agilent 7890A model GC and mass spectrometer (MS) with Agilent 5975C inert XL triaxial mass detector. The methods used in GC-MS and GC-ECD are described in detail in our other studies (Esen et al. 2010; Cindoruk 2011; Tasdemir et al. 2012; Esen 2013; Sari et al. 2020b, a). Briefly, the GC-MS oven program was; 50 °C (1 min) at the beginning, increased to 200 °C at 25 °C/min, followed by 8 °C/min up to 300 °C, and held at 300 °C (5.5 min), and 5 °C/min up to 310 °C (3 min). Helium was used as the carrier gas (1.4 mL/min). MS was performed in selected ion-monitoring mode (SIM). The purpose of this is to detect PAH compounds with a very high sensitivity of MS. The GC- $\mu\text{ECD}$  oven temperature program for PCB analysis was: 70 °C (2 min) at the beginning, increased to 150 °C at 25 °C/min, followed by increased to 200 °C at 3 °C/min, increased to 280 °C at 8 °C/min, 8 minutes standby at this temperature and finally increased to 300 °C at 10 °C/min and 2 minutes standby at this temperature. Similarly, GC- $\mu\text{ECD}$  oven temperature program for OCP analysis was: 80 °C (1 min), with increases of 20 °C/min to 240 °C, 5 minutes standby at

this temperature, followed by 5°C/min up to 270°C, then 20°C/min up to 300°C, 5 minutes standby at this temperature and finish. The injector inlet temperature was 250 °C, and the detector temperature was 320 °C (Cindoruk 2011; Sari et al. 2020a). Helium was used as the carrier gas (1.9 mL/min). High purity nitrogen gas was used as the make-up gas with helium gas. HP-5MS GC column (30m × 0.25mm × 0.25µm) was used as a capillary column in GC-MS, and HP-5 GC column (30 m × 0.32 mm × 0.25 µm) was used as a capillary column in GC-µECD. In this study, 14 PAH; Acenaphthene (Ace), Fluorene (Flu), Phenanthrene (Phe), Anthracene (Ant), Fluoranthene (Fl), Pyrene (Py), Benz(a)Anthracene (BaA), Chrysene (Chr), Benzo(b)Fluoranthene (BbF), Benzo(k)Fuoranthene (BkF), Benzo(a)Pyrene (BaP), Indeno(1,2,3-c,d)Pyrene (IcdP), Dibenz(a,h)Anthracene (DahA), and Benzo(g,h,i)Perylene (BghiP), 50 PCB; PCB#4/10, 6, 19, 12/13, 15/17, 31, 28, 22, 52, 44, 41/64/71, 74, 61/70, 66/95, 91, 56/60, 84, 99, 119, 81/87, 86, 135/144, 118, 123, 131, 153, 132/105, 138/163, 128, 174, 156/171/202, 172, 180, 199, 194 and 206, and 10 OCP; α-HCH, β-HCH, γ-HCH, δ-HCH, Heptachlor endo epoxide iso A, Endrin, Endosulfan-β, Endrin aldehyde, p,p'- DDT, and Methoxychlor were analysed. Of these compounds, Naphthalene and Acenaphthylene were not included in the calculations due to their low recovery efficiency (< 60%).

## 2.3. Quality Assurance /Quality Control (QA/QC)

Blank samples were used to check and prevent any possible contamination during the transportation of the PUFs, the extraction, or the quantification procedures. All glassware used during the preparation of samples, sampling, and laboratory analyzes were washed using tap water, distilled water, ACE, and PE, respectively. The surrogate standard was added to each sample before extraction for the determination of the analytical recovery efficiencies. Samples with recovery efficiency between 60% and 120% were included in the calculations. Surrogate standard consist of naphthalene-D8, acenaphthene-D10, phenanthrene-D10, chrysene-D12, and perylene-D12 (each 4000 ng) for PAHs; and PCB#14, PCB#65, and PCB#166 (each 4 ng) for PCBs. External recovery standard was used for OCPs, and not recovery-corrected was made since recovery efficiencies were generally higher than 70% (Cindoruk and Tasdemir 2014).

The GC-MS and GC-µECD instruments were calibrated before reading both blank and collected samples. Six level calibration standards were used for both instruments. Calibration standards were used for PAHs (0.2, 0.5, 1.0, 2.0, 5.0 and 10.0 µg/mL) and for PCBs and OCPs (0.5, 1.0, 2.0, 5.0, 10.0 and 20.0 ng/mL). The R<sup>2</sup> values of the calibration levels were higher than 0.99. The mid-level calibration standard was run to check the GC-MS and GC-µECD calibration requirements after every 100 samples. The limit of detection (LOD) and values were determined for individual POP compounds. The LOD values were calculated as the sum of the average blanks mass and three times the standard deviation (average + 3 std dev) (Sari et al. 2021). The instrument detection limits (IDLs) were calculated based on the lowest concentration of a calibration standard (Signal: Noise (S: N) ratio of 3:1). The IDL values for 1 µL injection were 0.1 ng for PAHs, 0.15 pg for PCBs and 0.04 pg for OCPs. The LOD values ranged from IDL to 30.48 ng for PAHs, from 0.26 to 9.18 pg for PCBs, and from 0.24 to 4.83 pg for OCPs. If the mass value of any POP compound is less than the LOD value, it was taken as half of that compound's IDL value for statistical analysis.

## 3. Results And Discussion

### 3.1. PAH concentrations and possible sources

The average concentrations of total 14 PAH ( $\sum_{14}\text{PAH}$ ) in the atmosphere were found to be  $54.4 \pm 22.6$  ng/m<sup>3</sup> (ranging from 24.4 to 91.3 ng/m<sup>3</sup>) and  $51.7 \pm 34.3$  ng/m<sup>3</sup> (ranging from 13.9 to 107.4 ng/m<sup>3</sup>) for the urban and semi-urban areas, respectively (Fig. 1a). The highest PAH concentrations were determined in December and January, while the lowest PAH concentrations in July and August in both sampling areas. In general, high PAH levels were measured in the winter months, which are associated with increased domestic heating. The low efficiency of fossil combustion reportedly increases PAH concentrations in the winter months (Albuquerque et al. 2016). The PAH concentrations measured in December, January and February in the semi-urban area were higher than in the urban area. Similar PAH concentrations were measured in both sampling areas from March and November (Fig. 1a). The semi-urban area is located on the mountainside, and for this reason, the weather is colder than the urban area. Therefore, fossil fuel is used earlier for domestic heating in semi-urban areas than in urban areas. In addition, there are more settlements in the semi-urban area than in the urban area. For these reasons, more fossil fuels are used in the months when the temperature drops. The PAH concentrations measured from April to October in the urban area were higher than in the semi-urban area. The high PAH concentrations measured in the urban area are explained by the fact that the region represents an area where industry and traffic are dense.

In this study, the seasonal PAH concentrations obtained for both sampling areas are shown in Fig. 1b. The seasonal distribution of  $\sum_{14}\text{PAH}$  concentrations ranged from 34.2 to 78.4 ng/m<sup>3</sup> for the urban area and ranged from 18.2 to 98.0 ng/m<sup>3</sup> for the semi-urban area. The highest PAH levels in both sampling areas were measured in the winter and autumn seasons, while the lowest PAH levels were measured in the spring and summer seasons. High atmospheric PAH concentrations measured in winter compared to summer are explained by local emission sources and increased long-range atmospheric transport. For example, using more fuel for heating during the winter months causes PAH concentrations to increase. In addition, meteorological factors are among the effective mechanisms on the temporal distribution of PAHs. Changes in ambient temperature play an important role in the absorption mechanisms and degradation of PAHs. Thus, higher PAH concentrations are measured in winter than in summer (Hong et al. 2020). Relatively PAH concentrations measured in winter and autumn have been attributed to lower temperatures, low solar radiation, low photo-degradation, and lower mixing height (Thang et al. 2020). Also, fossil fuels for domestic heating in winter and autumn increase PAH concentrations (Albuquerque et al. 2016). In this study, the concentrations obtained and both monthly and seasonal distributions were similar to those reported in other studies (Qin et al. 2013; Chen et al. 2014; Li et al. 2014, 2019; Albuquerque et al. 2016). The annual distributions of PAHs measured in the urban and semi-urban areas are shown in Fig. 1c. According to the annual distribution of PAH concentrations, there was a significant difference between the minimum and maximum concentrations in the semi-urban area compared to the urban area ( $p < 0.05$ ). This may be due to the fact that PAH sources in the urban area did not change

much throughout the year. In the semi-urban area, coal instead of natural gas, especially in winter, cause serious concentration differences between the summer and winter seasons. This situation creates differences in its annual distribution in the semi-urban area.

Molecular diagnostic ratios (MDRs) are the commonly used method for determining the sources of PAHs (Motelay-Massei et al. 2007). Many studies in the literature have used MDRs to determine the sources of PAHs in various environments (Katsoyiannis et al. 2007; Motelay-Massei et al. 2007). Among these rates,  $\text{Ant}/(\text{Ant} + \text{Phe})$ ,  $\text{Fl}/(\text{Fl} + \text{Py})$ ,  $\text{BaA}/(\text{BaA} + \text{Chr})$  and  $\text{IcdP}/(\text{IcdP} + \text{BghiP})$  ratios are mostly used to determine the sources of PAHs in the literature (Katsoyiannis et al. 2007; Motelay-Massei et al. 2007; Tobiszewski and Namieśnik 2012; Sari et al. 2020b).  $\text{Ant}/(\text{Ant} + \text{Phe})$  ratios are often used to distinguish combustion or petroleum emissions. If the  $\text{Ant}/(\text{Ant} + \text{Phe})$  ratio is higher than 0.1, it means that high temperatures ( $> 800\text{ }^{\circ}\text{C}$ ) are effective in the formation of PAH, and if this ratio is less than 0.1, PAHs are usually produced by chemical reactions at both slow and lower temperatures (Chen et al. 2020b).  $\text{Fl}/(\text{Fl} + \text{Py})$ ,  $\text{BaA}/(\text{BaA} + \text{Chr})$  and  $\text{IcdP}/(\text{IcdP} + \text{BghiP})$  ratios are used to distinguish petroleum and combustion emissions. If the  $\text{Fl}/(\text{Fl} + \text{Py})$  ratio is less than 0.4, it refers to petroleum sources and if it is greater than 0.5, it refers to combustion sources. This ratio shows that mixed sources (liquid fossil fuel combustion) are effective between 0.4–0.5 (He et al. 2014; Sari et al. 2020b; Wang et al. 2020a). Similarly, if the  $\text{BaA}/(\text{BaA} + \text{Chr})$  ratio is less than 0.2, PAHs are generally produced by petrogenic emissions, and if this ratio is greater than 0.35, it refers to combustion sources. Similar situations apply for  $\text{IcdP}/(\text{IcdP} + \text{BghiP})$  ratios. “The combustion-derived PAHs (COMPAHs) is defined as a combination including Fl, Py, BaA, Chr, BbF, BkF, BaP, IcdP, and BghiP” (Li et al. 2016). The positive correlation between COMPAH and total PAH concentrations means that combustion is the dominant source (He et al. 2014). The MDR values and the correlation results between COMPAH and total PAH obtained in this study are shown in Fig. 2.

The  $\text{Ant}/(\text{Ant} + \text{Phe})$  ratios in the urban area were calculated as higher than 0.1. This meant that PAHs in this area were formed at high temperatures. In this case, it is consistent with the fact that this area represents a region where the industry is dense. In general, coal and biomass combustion emissions are dominant in both areas according to both  $\text{Fl}/(\text{Fl} + \text{Py})$  and  $\text{BaA}/(\text{BaA} + \text{Chr})$  ratios. Similarly,  $\text{IcdP}/(\text{IcdP} + \text{BghiP})$  ratios are often higher than 0.4 for urban and semi-urban areas. Also, high correlation levels between COMPAH and total PAH concentrations meant that combustion sources were dominant (He et al. 2014). The correlation between COMPAH and total PAH was strong, with a correlation coefficient of  $R = 0.97$  (in the urban area) and  $R = 0.94$  (in the semi-urban area). According to both MDR and correlation results between COMPAH and Total PAH, combustion sources dominated in both areas. Combustion sources in the urban area occurred at high temperatures ( $> 800\text{ }^{\circ}\text{C}$ ) originating from industry ( $(\text{Ant}/(\text{Ant} + \text{Phe})) > 0.1$ ), while in the semi-urban area, it was usually caused by the combustion of petrogenic-derived fuels.

## 3.2. PCB concentrations and possible sources

The mean monthly concentrations of total 50 PCBs ( $\sum_{50}\text{PCBs}$ ) in the atmosphere were found to be  $522.5 \pm 196.9\text{ pg}/\text{m}^3$  (ranging from 271.4 to 826.6  $\text{pg}/\text{m}^3$ ) and  $439.5 \pm 166.6\text{ pg}/\text{m}^3$  (ranging from 243.2

to 727.2 pg/m<sup>3</sup>) for the urban and semi-urban areas, respectively (Fig. 3a). Several studies have recently reported the PCB concentration in ambient air in Bursa (Cindoruk et al. 2007, 2020; Günindi and Tasdemir 2010; Tasdemir et al. 2012; Birgül et al. 2017; Sari et al. 2020a). The concentrations obtained in this study are similar to those reported in the literature (Cindoruk et al. 2007, 2020; Günindi and Tasdemir 2010; Tasdemir et al. 2012; Aydin et al. 2014; Birgül et al. 2017; Sari et al. 2020a).

The highest PCB concentrations were determined in June, while the lowest PCB concentrations were determined in March in the urban area. In the semi-urban area, the highest concentration of PCBs occurred in July, while the lowest concentrations were determined in November. Due to the evaporation of PCBs at high temperatures, atmospheric levels also increase in the summer months (Ozcan and Aydin 2009). Therefore, evaporation may have been effective at high PCB levels measured in the summer months in both sampling areas. Considering the seasonal distribution of PCBs, the highest concentrations were measured in summer, while the lowest concentration levels were measured in autumn and winter at both sampling areas (Fig. 3b). The atmospheric input of PCBs reaches maximum levels in the summer due to the evaporation of congeners from hot ambient conditions (Hogarh et al. 2013). Similar results were obtained in most studies on PCBs in the literature (Cindoruk et al. 2007; Ozcan and Aydin 2009; Hogarh et al. 2013; Aydin et al. 2014; Birgül et al. 2017). For this reason, the maximum PCB concentrations observed in the summer in this study are consistent with studies in the literature. The annual distributions of PCBs measured in the urban and semi-urban areas are shown in Fig. 3c. Considering the annual distribution of PCBs, higher concentrations were observed in the urban area. Some of the factors that have been reported in the literature as having contributed to contemporary levels of PCBs in the environment include improper storage of PCB-containing waste, incineration of municipal or industrial wastes, evaporation from contaminated surfaces, accidental disposal of PCB-containing waste, and old electronic equipment used (Aydin et al. 2014). As the urban area is close to industry, annual PCBs were found to be higher than in the semi-urban area.

Homologs groups of PCBs in the air samples generally provide information about transport, possible sources, and fate (Habibullah-Al-Mamun et al. 2019). For example, if high homologs group PCBs are dominant in one area, uses of technical PCB mixtures may prevail locally. On the other hand, if low homologs group PCBs are dominant in an area, long-range transport and secondary emissions source factors may be dominant (Birgül et al. 2017). Moreover, the differences between homologous groups are due to physicochemical differences between PCB congeners with different chlorine numbers (Hu et al. 2019). In this study, seasonally calculated homologs group distributions for the urban and semi-urban areas are shown in Fig. 4.

Penta- (ranging from 21.1–28.6%) and Tri- (ranging from 18.3–22.2%) chlorinated PCBs formed dominant homologs groups in the urban area. Similarly, Penta- (ranging from 25.2–29.1%) chlorinated PCBs were predominant in all seasons in the semi-urban area. Also, Tetra- (ranging from 16.9–19.8%) chlorinated PCBs are predominant in the spring, summer, and autumn seasons in the semi-urban area (Fig. 4). High chlorinated PCBs (Hepta-, Octa-, and Nona-CBs) were not dominant in both sampling areas. This situation could be explained by collecting the gas phase chemicals by diffusion with the PUF-disk

sampler (Birgül et al. 2017). A study conducted by Sari et al. (2020a) reported that Penta- (37%) and Tetra- (22%) chlorinated PCBs were the dominant homologs group for Bursa in 2014. Another study conducted by Birgül et al. (2017) reported that Tetra-(31.5–81.6%) chlorinated PCBs were the dominant homolog groups for Bursa in 2014. Cindoruk and Tasdemir (2007) also reported that Tri- (64.6%) and Tetra-(22.9%) chlorinated PCBs were the dominant homologs group for Bursa in 2005.

Especially in the summer months, PCBs evaporating with the increase of the temperature increase the ambient air concentrations (Hogarh et al. 2013). With the increase of temperature in summer in both sampling areas, Di-chlorinated PCBs became dominant. Because of the low saturated vapour pressure of the low chlorinated PCBs, they are more likely to be moved from a source to more distant areas than high-chlorinated PCBs (Hu et al. 2019). For this reason, atmospheric transport in summer is also thought to affect PCB concentrations.

### 3.3. OCP concentrations and possible sources

The mean monthly concentrations of a total of 10 OCPs ( $\sum_{10} \text{OCPs}$ ) were found to be  $242.5 \pm 104.6$   $\text{pg/m}^3$  (ranging from 105.3 to 448.6  $\text{pg/m}^3$ ) and  $275.9 \pm 130.9$   $\text{pg/m}^3$  (ranging from 104.8 to 546.4  $\text{pg/m}^3$ ) for the urban and semi-urban areas, respectively. The concentrations obtained in this study were consistent with reported studies in the literature (Batterman et al. 2008; Yang et al. 2008; Syed et al. 2013; Zhang et al. 2013; Gevao et al. 2018). The highest concentrations were observed in June, while the lowest concentrations were observed in April in both sampling areas (Fig. 5a). Regarding the seasonal distribution of OCPs, the highest concentrations were observed in the summer season, while the lowest levels were observed in the spring season (Fig. 5b). High OCP concentrations seen in the summer season can be explained by increasing agricultural activities in this season (Qu et al. 2015). According to the annual distribution of OCP concentrations, higher levels were determined in the semi-urban area compared to the urban area (Fig. 5c). This situation is consistent with the fact that agricultural activities are more in a semi-urban area.

Hexachlorocyclohexanes (HCHs) were among the most common pesticides produced for agricultural use worldwide between the 1950s and 1980s (Balázs et al. 2018). Technical HCHs are compounds containing about  $\alpha$ -HCH (60–70 %),  $\beta$ -HCH (5–12%),  $\gamma$ -HCH (10–15%),  $\delta$ -isomer (6–10%) and very low amounts of other isomers (Garmouma and Poissant 2004; Sun et al. 2016). These isomers have different physical and chemical properties. For example, while  $\alpha$ -HCH can be transported over long distances in the atmosphere,  $\beta$ -HCH is more resistant to environmental degradation and hydrolysis (Da et al. 2014). Among the HCH isomers,  $\gamma$ -HCHs, also known as lindane, form the most active group and are often used as insecticides (Yang et al. 2018). During the sampling period, total HCH (sum of  $\alpha$ -,  $\beta$ -,  $\gamma$ -, and  $\delta$ -) concentrations were found as  $141.5 \pm 65.0$   $\text{pg/m}^3$  for the urban area and  $189.8 \pm 111.1$   $\text{pg/m}^3$  for the semi-urban area. Thus,  $\beta$ -HCH is the dominant HCH isomer in both sampling areas. In previous studies in Bursa,  $\beta$ -HCH was reported to be the dominant HCH isomer (Cindoruk 2011; Esen 2013), possibly due to atmospheric transport from contaminated areas and evaporation from vegetation (Cindoruk 2011).

The ratios of  $\alpha$ -HCH/ $\gamma$ -HCH and  $\beta/(\alpha + \gamma)$ -HCH are often used in source identification of HCHs (Kong et al. 2014). For example, if the  $\alpha$ -HCH/ $\gamma$ -HCH ratio is less than 4, lindane is dominant, whereas if the  $\alpha$ -HCH/ $\gamma$ -HCH ratio is between 4–7, technical HCHs are dominant (Da et al. 2014). Similarly, if the  $\beta/(\alpha + \gamma)$ -HCH ratio is higher than 0.5, it means that the pesticide has been used in the past, and if the ratio is less than 0.5, then the pesticide has been used recently (Liu et al. 2012). In this study,  $\alpha$ -HCH/ $\gamma$ -HCH and  $\beta/(\alpha + \gamma)$ -HCH ratios calculated for urban and semi-urban areas are shown in Fig. 6.

The mean  $\alpha$ -HCH/ $\gamma$ -HCH ratios were found to be 0.87 for the urban area and 1.15 for the semi-urban area. According to the  $\alpha$ -HCH/ $\gamma$ -HCH ratios, lindane was predominant in both sampling areas. A study conducted by Cindoruk (2011) in Bursa stated that  $\alpha$ -HCH/ $\gamma$ -HCH ratios are generally higher than 1.0. In another study conducted in Bursa,  $\alpha$ -HCH/ $\gamma$ -HCH ratios were reported to vary between 0.27–0.55 (Esen 2013). A study conducted by Kurt-Karakus et al. (2018) across Turkey reported the average  $\alpha$ -HCH/ $\gamma$ -HCH ratios as 2.26 for the urban area. Although these compounds have long been banned, it is thought that high concentrations of  $\gamma$ -HCHs are reintroduced into the atmosphere through illicit use, pure lindane use and evaporation from formerly contaminated areas (Cindoruk 2011). According to  $\beta/(\alpha + \gamma)$ -HCH ratios, most the pesticides have been used recently. In a study by Wu et al. (2020), they stated that until 2019, lindane was used to control termites in China, while in Japan, it was still used for wood preservatives. It can also be explained that high lindane levels are still used in many countries even though they are banned (Yang et al. 2008).

## 4. Conclusions

In this study, concentration levels, temporal and spatial variations, and possible sources of POPs such as PAHs, PCBs, and OCPs were determined using a passive air sampler in urban and semi-urban areas for 12 months. The average annual PAH and PCB concentrations were higher in the urban area, while OCP concentrations were higher in the semi-urban area. Industrial and traffic activities were effective in the urban area, while agricultural activities were generally effective in the semi-urban area. Combustion was the primary source of PAHs in both sampling areas. Combustion sources in the urban area occur at high temperatures ( $> 800$  °C) originating from industry ( $(\text{Ant}/(\text{Ant} + \text{Phe}) > 0.1)$ ), while in the semi-urban area, it is usually caused by the combustion of petrogenic-derived fuels. Low chlorinated PCBs (Tri-, Tetra-, and Penta- chlorinated PCBs) were dominant in both sampling areas. This situation was explained by the collecting of the gas phase chemicals by diffusion with the PUF-disk sampler. Isomer distributions of HCHs were used to determine the sources of OCPs. According to the  $\alpha$ -HCH/ $\gamma$ -HCH ratios, lindane was determined to be effective in both sampling areas. Also,  $\beta/(\alpha + \gamma)$ -HCH ratios were determined higher in urban areas than in semi-urban areas. According to this result, most of the pesticides were used recently in the semi-urban area.

## Declarations

### Ethics approval and consent to participate

Not Applicable

## Consent for publication

Not Applicable

## Availability of data and materials

The datasets used and/or analysed during the current study are available from the corresponding author on reasonable request.

## Competing interests

The authors declare that they have no known competing financial interests or personal relationships that could have appeared to influence the work reported in this paper.

## Funding

This study was supported by the Turkish Scientific and Technological Research Council (TÜBİTAK) (project number 116Y208) and the Bursa Uludag University Scientific Research Projects, Turkey (Project No: OUAP (MH)-2020/8).

## Authors' contributions

**Mehmet Ferhat Sari:** Methodology, Software, Formal analysis, Writing - Original Draft, Data Curation.

**Fatma Esen:** Methodology, Data Curation, Writing - Original Draft, Writing - Review & Editing, Visualization, Supervision.

## References

1. Albuquerque M, Coutinho M, Borrego C (2016) Long-term monitoring and seasonal analysis of polycyclic aromatic hydrocarbons (PAHs) measured over a decade in the ambient air of Porto, Portugal. *Sci Total Environ* 543:439–448. <https://doi.org/10.1016/j.scitotenv.2015.11.064>
2. Amador-Muñoz O, Martínez-Domínguez YM, Gómez-Arroyo S, Peralta O (2020) Current situation of polycyclic aromatic hydrocarbons (PAH) in PM<sub>2.5</sub> in a receptor site in Mexico City and estimation of carcinogenic PAH by combining non-real-time and real-time measurement techniques. *Sci Total Environ* 703:134526. <https://doi.org/10.1016/j.scitotenv.2019.134526>
3. Aydin YM, Kara M, Dumanoglu Y et al (2014) Source apportionment of polycyclic aromatic hydrocarbons (PAHs) and polychlorinated biphenyls (PCBs) in ambient air of an industrial region in Turkey. *Atmos Environ* 97:271–285. <https://doi.org/10.1016/j.atmosenv.2014.08.032>
4. Balázs EH, Schmid CAO, Feher I et al (2018) HCH phytoremediation potential of native plant species from a contaminated urban site in Turda, Romania. *J Environ Manage* 223:286–296.

- <https://doi.org/10.1016/j.jenvman.2018.06.018>
5. Batterman SA, Chernyak SM, Gounden Y et al (2008) Organochlorine pesticides in ambient air in Durban, South Africa. *Sci Total Environ* 397:119–130.  
<https://doi.org/10.1016/j.scitotenv.2008.02.033>
  6. Birgül A, Kurt-Karakus PB, Alegria H et al (2017) Polyurethane foam (PUF) disk passive samplers derived polychlorinated biphenyls (PCBs) concentrations in the ambient air of Bursa-Turkey: Spatial and temporal variations and health risk assessment. *Chemosphere* 168:1345–1355.  
<https://doi.org/10.1016/j.chemosphere.2016.11.124>
  7. Chen CF, Ju YR, Su YC et al (2020a) Distribution, sources, and behavior of PAHs in estuarine water systems exemplified by Salt River, Taiwan. *Mar Pollut Bull* 154:.  
<https://doi.org/10.1016/j.marpolbul.2020.111029>
  8. Chen D, Grimsrud TK, Langseth H et al (2020b) Prediagnostic serum concentrations of organochlorine pesticides and non-Hodgkin lymphoma: A nested case–control study in the Norwegian Janus Serum Bank Cohort. *Environ Res* 187:109515.  
<https://doi.org/10.1016/j.envres.2020.109515>
  9. Chen Y, Cao J, Zhao J et al (2014) N-Alkanes and polycyclic aromatic hydrocarbons in total suspended particulates from the southeastern Tibetan Plateau: Concentrations, seasonal variations, and sources. *Sci Total Environ* 470–471:9–18. <https://doi.org/10.1016/j.scitotenv.2013.09.033>
  10. Cindoruk SS (2011) Atmospheric organochlorine pesticide (OCP) levels in a metropolitan city in Turkey. *Chemosphere* 82:78–87. <https://doi.org/10.1016/j.chemosphere.2010.10.003>
  11. Cindoruk SS, Esen F, Tasdemir Y (2007) Concentration and gas/particle partitioning of polychlorinated biphenyls (PCBs) at an industrial site at Bursa, Turkey. *Atmos Res* 85:338–350.  
<https://doi.org/10.1016/j.atmosres.2007.02.004>
  12. Cindoruk SS, Sakin AE, Tasdemir Y (2020) Levels of persistent organic pollutants in pine tree components and ambient air. *Environ Pollut* 256:.  
<https://doi.org/10.1016/j.envpol.2019.113418>
  13. Cindoruk SS, Tasdemir Y (2014) The investigation of atmospheric deposition distribution of organochlorine pesticides (OCPs) in Turkey. *Atmos Environ* 87:207–217.  
<https://doi.org/10.1016/j.atmosenv.2014.01.008>
  14. Cindoruk SS, Tasdemir Y (2007) The determination of gas phase dry deposition fluxes and mass transfer coefficients (MTCs) of polychlorinated biphenyls (PCBs) using a modified water surface sampler (WSS). *Sci Total Environ* 381:212–221. <https://doi.org/10.1016/j.scitotenv.2007.03.011>
  15. Da C, Liu G, Yuan Z (2014) Analysis of HCHs and DDTs in a sediment core from the Old Yellow River Estuary, China. *Ecotoxicol Environ Saf* 100:171–177. <https://doi.org/10.1016/j.ecoenv.2013.10.034>
  16. Esen F (2013) Development of a Passive Sampling Device Using Polyurethane Foam (PUF) to Measure Polychlorinated Biphenyls (PCBs) and Organochlorine Pesticides (OCPs) near Landfills. *Environ Forensics* 14:1–8. <https://doi.org/10.1080/15275922.2012.729008>
  17. Esen F, Tasdemir Y, Siddik Cindoruk S (2010) Determination of mass transfer rates and deposition levels of polycyclic aromatic hydrocarbons (PAHs) using a modified water surface sampler. *Atmos*

- Pollut Res 1:177–183. <https://doi.org/10.5094/APR.2010.023>
18. Estellano VH, Pozo K, Příbylová P et al (2017) Assessment of seasonal variations in persistent organic pollutants across the region of Tuscany using passive air samplers. *Environ Pollut* 222:609–616. <https://doi.org/10.1016/j.envpol.2016.08.092>
  19. Garmouma M, Poissant L (2004) Occurrence, temperature and seasonal trends of  $\alpha$ - and  $\gamma$ -HCH in air (Québec, Canada). *Atmos Environ* 38:369–382. <https://doi.org/10.1016/j.atmosenv.2003.10.007>
  20. Gaurav GK, Mehmood T, Kumar M et al (2021) Review on polycyclic aromatic hydrocarbons (PAHs) migration from wastewater. *J Contam Hydrol* 236:103715. <https://doi.org/10.1016/j.jconhyd.2020.103715>
  21. Gevao B, Porcelli M, Rajagopalan S et al (2018) Spatial and temporal variations in the atmospheric concentrations of “Stockholm Convention” organochlorine pesticides in Kuwait. *Sci Total Environ* 622–623:1621–1629. <https://doi.org/10.1016/j.scitotenv.2017.10.036>
  22. Günindi M, Tasdemir Y (2010) Atmospheric polychlorinated biphenyl (pcb) inputs to a coastal city near the marmara sea. *Mar Pollut Bull* 60:2242–2250. <https://doi.org/10.1016/j.marpolbul.2010.08.012>
  23. Habibullah-Al-Mamun M, Kawser Ahmed M, Saiful Islam M et al (2019) Occurrence, distribution and possible sources of polychlorinated biphenyls (PCBs) in the surface water from the Bay of Bengal coast of Bangladesh. *Ecotoxicol Environ Saf* 167:450–458. <https://doi.org/10.1016/j.ecoenv.2018.10.052>
  24. He J, Fan S, Meng Q et al (2014) Polycyclic aromatic hydrocarbons (PAHs) associated with fine particulate matters in Nanjing, China: Distributions, sources and meteorological influences. *Atmos Environ* 89:207–215. <https://doi.org/10.1016/j.atmosenv.2014.02.042>
  25. Herkert NJ, Martinez A, Hornbuckle KC (2016) A Model Using Local Weather Data to Determine the Effective Sampling Volume for PCB Congeners Collected on Passive Air Samplers. *Environ Sci Technol* 50:6690–6697. <https://doi.org/10.1021/acs.est.6b00319>
  26. Hogarh JN, Seike N, Kobara Y, Masunaga S (2013) Seasonal variation of atmospheric polychlorinated biphenyls and polychlorinated naphthalenes in Japan. *Atmos Environ* 80:275–280. <https://doi.org/10.1016/j.atmosenv.2013.07.076>
  27. Hong WJ, Jia H, Yang M, Li YF (2020) Distribution, seasonal trends, and lung cancer risk of atmospheric polycyclic aromatic hydrocarbons in North China: A three-year case study in Dalian city. *Ecotoxicol Environ Saf* 196:110526. <https://doi.org/10.1016/j.ecoenv.2020.110526>
  28. Hu J, Wu J, Xu C et al (2019) Preliminary investigation of polychlorinated dibenzo-p-dioxin and dibenzofuran, polychlorinated naphthalene, and dioxin-like polychlorinated biphenyl concentrations in ambient air in an industrial park at the northeastern edge of the Tibet–Qinghai Plateau. *Sci Total Environ* 648:935–942. <https://doi.org/10.1016/j.scitotenv.2018.08.241>
  29. Ji X, Abakumov E, Polyako V et al (2019) The ecological impact of mineral exploitation in the Russian Arctic: A field-scale study of polycyclic aromatic hydrocarbons (PAHs) in permafrost-

- affected soils and lichens of the Yamal-Nenets autonomous region. *Environ Pollut* 255:113239. <https://doi.org/10.1016/j.envpol.2019.113239>
30. Katsoyiannis A, Terzi E, Cai QY (2007) On the use of PAH molecular diagnostic ratios in sewage sludge for the understanding of the PAH sources. Is this use appropriate? *Chemosphere* 69:1337–1339. <https://doi.org/10.1016/j.chemosphere.2007.05.084>
  31. Kong X, He W, Qin N et al (2014) Modeling the multimedia fate dynamics of  $\gamma$ -hexachlorocyclohexane in a large Chinese lake. *Ecol Indic* 41:65–74. <https://doi.org/10.1016/j.ecolind.2014.01.024>
  32. Li Q, Jiang N, Yu X et al (2019) Sources and spatial distribution of PM<sub>2.5</sub>-bound polycyclic aromatic hydrocarbons in Zhengzhou in 2016. *Atmos Res* 216:65–75. <https://doi.org/10.1016/j.atmosres.2018.09.011>
  33. Li W, Wang C, Wang H et al (2014) Atmospheric polycyclic aromatic hydrocarbons in rural and urban areas of northern China. *Environ Pollut* 192:83–90. <https://doi.org/10.1016/j.envpol.2014.04.039>
  34. Li X, Kong S, Yin Y et al (2016) Polycyclic aromatic hydrocarbons (PAHs) in atmospheric PM<sub>2.5</sub> around 2013 Asian Youth Games period in Nanjing. *Atmos Res* 174–175:85–96. <https://doi.org/10.1016/j.atmosres.2016.01.010>
  35. Liu WX, He W, Qin N et al (2012) Residues, distributions, sources, and ecological risks of ocp's in the water from Lake Chaohu, China. *Sci World J* 2012:.. <https://doi.org/10.1100/2012/897697>
  36. Motelay-Massei A, Ollivon D, Garban B et al (2007) PAHs in the bulk atmospheric deposition of the Seine river basin: Source identification and apportionment by ratios, multivariate statistical techniques and scanning electron microscopy. *Chemosphere* 67:312–321. <https://doi.org/10.1016/j.chemosphere.2006.09.074>
  37. Naing NN, Yeo K, Bin, Lee HK (2020) A combined microextraction procedure for isolation of polycyclic aromatic hydrocarbons in ambient fine air particulate matter with determination by gas chromatography-tandem mass spectrometry. *J Chromatogr A* 1612:460646. <https://doi.org/10.1016/j.chroma.2019.460646>
  38. Ontiveros-Cuadras JF, Ruiz-Fernández AC, Sanchez-Cabeza JA et al (2019) Recent history of persistent organic pollutants (PAHs, PCBs, PBDEs) in sediments from a large tropical lake. *J Hazard Mater* 368:264–273. <https://doi.org/10.1016/j.jhazmat.2018.11.010>
  39. Ozcan S, Aydin ME (2009) Polycyclic aromatic hydrocarbons, polychlorinated biphenyls and organochlorine pesticides in urban air of Konya, Turkey. *Atmos Res* 93:715–722. <https://doi.org/10.1016/j.atmosres.2009.02.012>
  40. Qin N, He W, Kong XZ et al (2013) Atmospheric partitioning and the air-water exchange of polycyclic aromatic hydrocarbons in a large shallow Chinese lake (Lake Chaohu). *Chemosphere* 93:1685–1693. <https://doi.org/10.1016/j.chemosphere.2013.05.038>
  41. Qu C, Albanese S, Lima A et al (2019) The occurrence of OCPs, PCBs, and PAHs in the soil, air, and bulk deposition of the Naples metropolitan area, southern Italy: Implications for sources and environmental processes. *Environ Int* 124:89–97. <https://doi.org/10.1016/j.envint.2018.12.031>

42. Qu C, Xing X, Albanese S et al (2015) Spatial and seasonal variations of atmospheric organochlorine pesticides along the plain-mountain transect in central China: Regional source vs. long-range transport and air-soil exchange. *Atmos Environ* 122:31–40.  
<https://doi.org/10.1016/j.atmosenv.2015.09.008>
43. Ruggeri MF, Lana NB, Altamirano JC, Puliafito SE (2020) Spatial distribution, patterns and source contributions of POPs in the atmosphere of Great Mendoza using the WRF/CALMET/CALPUFF modelling system. *Emerg Contam* 6:103–113. <https://doi.org/10.1016/j.emcon.2020.02.002>
44. Sah R, Baroth A, Hussain SA (2020) First account of spatio-temporal analysis, historical trends, source apportionment and ecological risk assessment of banned organochlorine pesticides along the Ganga River. *Environ Pollut* 263:114229. <https://doi.org/10.1016/j.envpol.2020.114229>
45. Sari MF, Esen F, Cordova Del Aguila DA, Kurt Karakus PB (2020a) Passive sampler derived polychlorinated biphenyls (PCBs) in indoor and outdoor air in Bursa, Turkey: Levels and an assessment of human exposure via inhalation. *Atmos Pollut Res*.  
<https://doi.org/10.1016/j.apr.2020.03.001>
46. Sari MF, Esen F, Tasdemir Y (2020b) Biomonitoring and Source Identification of Polycyclic Aromatic Hydrocarbons (PAHs) Using Pine Tree Components from Three Different Sites in Bursa, Turkey. *Arch Environ Contam Toxicol*. <https://doi.org/10.1007/s00244-020-00722-1>
47. Sari MF, Esen F, Tasdemir Y (2021) Levels of polychlorinated biphenyls (PCBs) in honeybees and bee products and their evaluation with ambient air concentrations. *Atmos Environ* 244:117903.  
<https://doi.org/10.1016/j.atmosenv.2020.117903>
48. Sun Y, Liang Z, Xiang X et al (2016) Simulation of the transfer and fate of  $\gamma$ -HCH in epikarst system. *Chemosphere* 148:255–262. <https://doi.org/10.1016/j.chemosphere.2015.10.091>
49. Syed JH, Malik RN, Liu D et al (2013) Organochlorine pesticides in air and soil and estimated air-soil exchange in Punjab, Pakistan. *Sci Total Environ* 444:491–497.  
<https://doi.org/10.1016/j.scitotenv.2012.12.018>
50. Tasdemir Y, Salihoglu G, Salihoglu NK, Birgül A (2012) Air-soil exchange of PCBs: Seasonal variations in levels and fluxes with influence of equilibrium conditions. *Environ Pollut* 169:90–97.  
<https://doi.org/10.1016/j.envpol.2012.05.022>
51. Thang PQ, Kim SJ, Lee SJ et al (2020) Monitoring of polycyclic aromatic hydrocarbons using passive air samplers in Seoul, South Korea: Spatial distribution, seasonal variation, and source identification. *Atmos Environ* 229:117460. <https://doi.org/10.1016/j.atmosenv.2020.117460>
52. Tobiszewski M, Namieśnik J (2012) PAH diagnostic ratios for the identification of pollution emission sources. *Environ Pollut* 162:110–119. <https://doi.org/10.1016/j.envpol.2011.10.025>
53. Wang S, Ji Y, Zhao J et al (2020a) Source apportionment and toxicity assessment of PM<sub>2.5</sub>-bound PAHs in a typical iron-steel industry city in northeast China by PMF-ILCR. *Sci Total Environ* 713:136428. <https://doi.org/10.1016/j.scitotenv.2019.136428>
54. Wang S, Zhang S, Huang H et al (2011) Uptake, translocation and metabolism of polybrominated diphenyl ethers (PBDEs) and polychlorinated biphenyls (PCBs) in maize (*Zea mays* L.). *Chemosphere*

- 85:379–385. <https://doi.org/10.1016/j.chemosphere.2011.07.002>
55. Wang X, Gong P, Wang C et al (2020b) Spatial distribution patterns and human exposure risks of polycyclic aromatic hydrocarbons, organochlorine pesticides and polychlorinated biphenyls in Nepal using tree bark as a passive air sampler. *Environ Res* 186:109510. <https://doi.org/10.1016/j.envres.2020.109510>
56. Wu Z, Lin T, Hu L et al (2020) Atmospheric legacy organochlorine pesticides and their recent exchange dynamics in the Northwest Pacific Ocean. *Sci Total Environ* 727:138408. <https://doi.org/10.1016/j.scitotenv.2020.138408>
57. Yang J, Shen F, Qiu M, Qi X (2018) Catalytic dehydrochlorination of lindane by nitrogen-containing multiwalled carbon nanotubes (N-MWCNTs). *Sci Total Environ* 621:1445–1452. <https://doi.org/10.1016/j.scitotenv.2017.10.084>
58. Yang Y, Li D, Mu D (2008) Levels, seasonal variations and sources of organochlorine pesticides in ambient air of Guangzhou, China. *Atmos Environ* 42:677–687. <https://doi.org/10.1016/j.atmosenv.2007.09.061>
59. Zhang C, Li Y, Wang C et al (2020a) Polycyclic aromatic hydrocarbons (PAHs) in marine organisms from two fishing grounds, South Yellow Sea, China: Bioaccumulation and human health risk assessment. *Mar Pollut Bull* 153:110995. <https://doi.org/10.1016/j.marpolbul.2020.110995>
60. Zhang L, Dong L, Yang W et al (2013) Passive air sampling of organochlorine pesticides and polychlorinated biphenyls in the Yangtze River Delta, China: Concentrations, distributions, and cancer risk assessment. *Environ Pollut* 181:159–166. <https://doi.org/10.1016/j.envpol.2013.06.033>
61. Zhang L, Yang L, Zhou Q et al (2020b) Size distribution of particulate polycyclic aromatic hydrocarbons in fresh combustion smoke and ambient air: A review. *J Environ Sci (China)* 88:370–384. <https://doi.org/10.1016/j.jes.2019.09.007>

## Figures

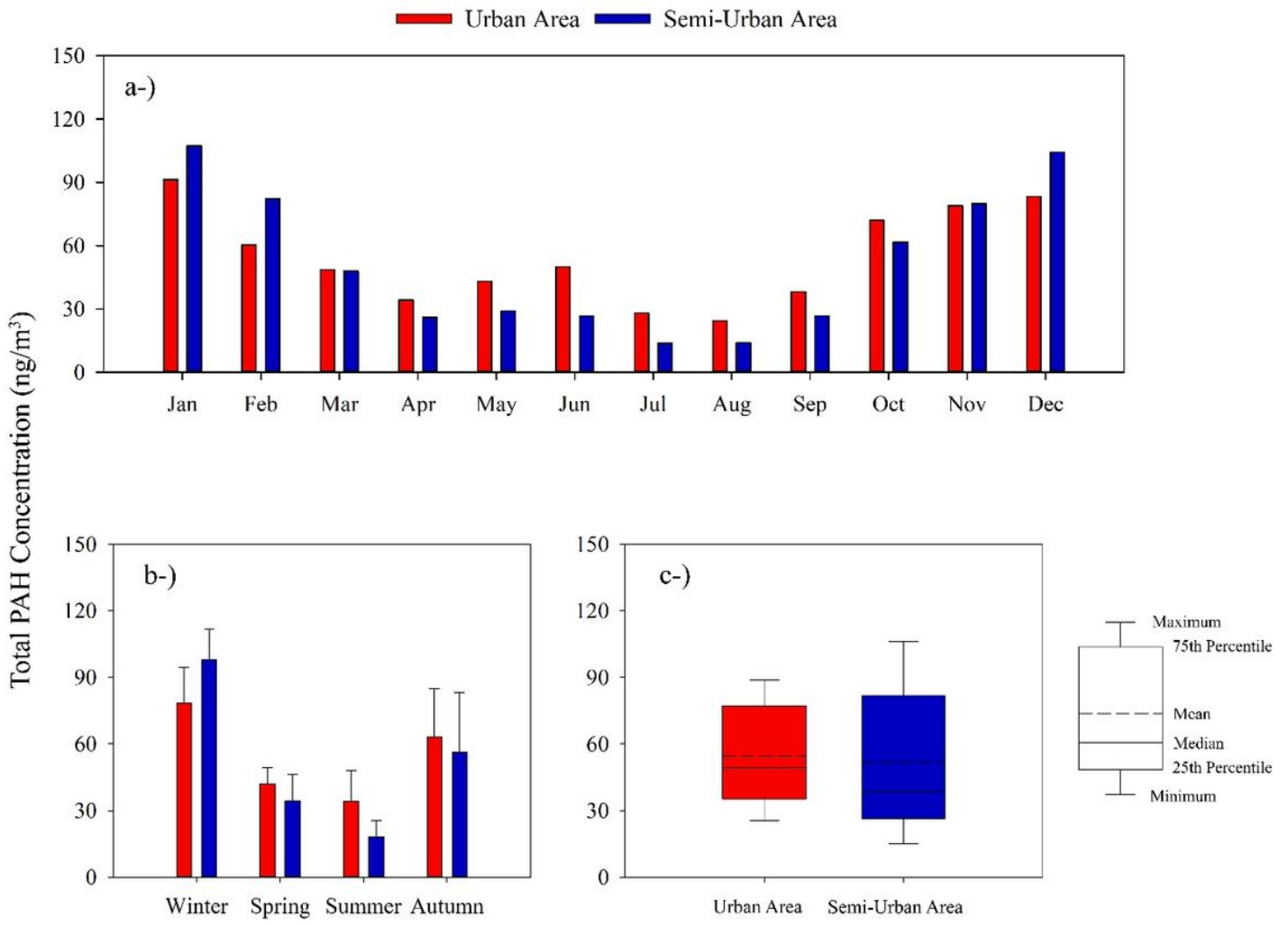


**Figure 1**

Monthly (a), seasonal (b) and annual (c) PAH distributions for the sampling areas

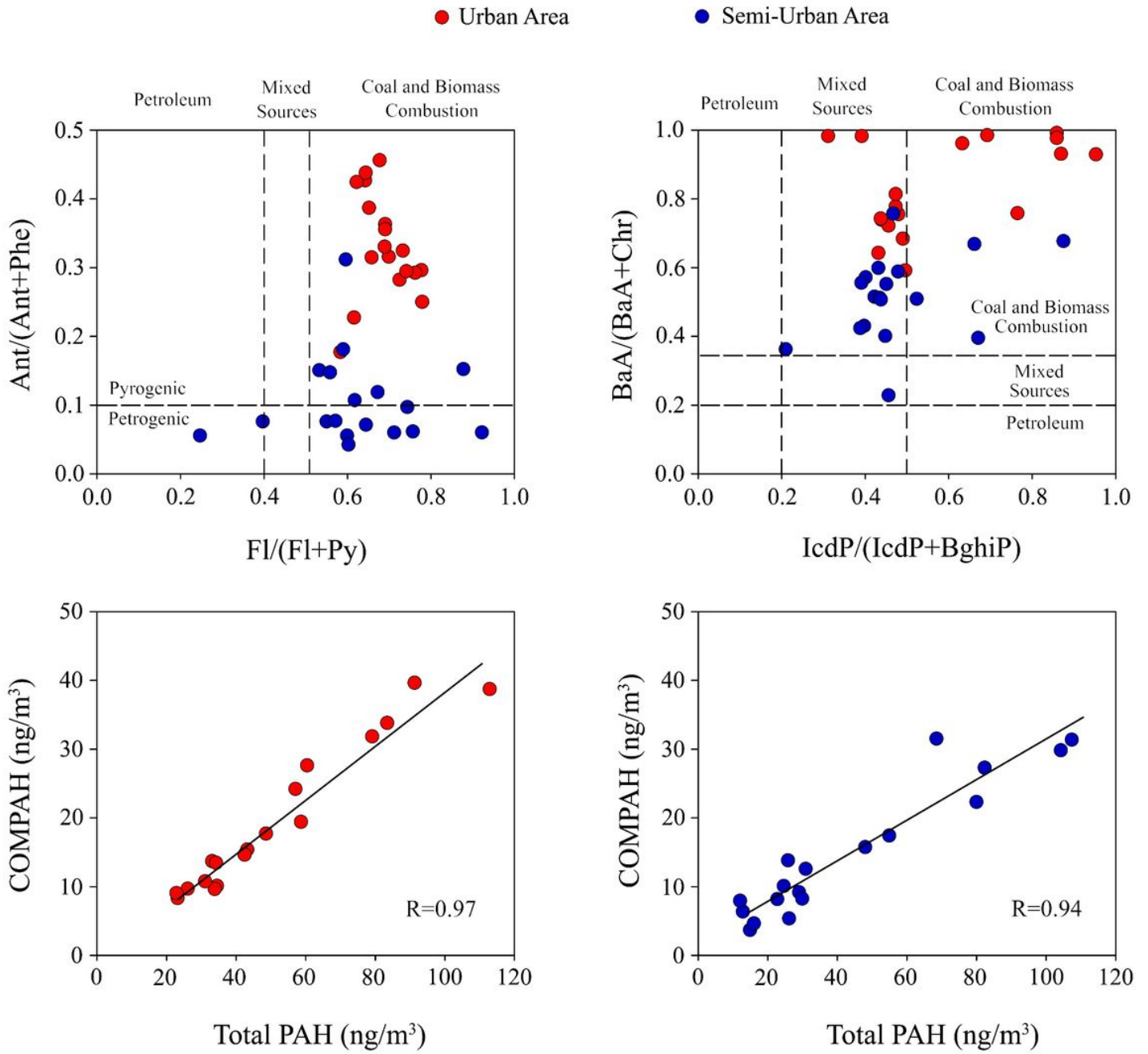


**Figure 2**

The MDR values and the correlation results between COMPAH and Total PAH

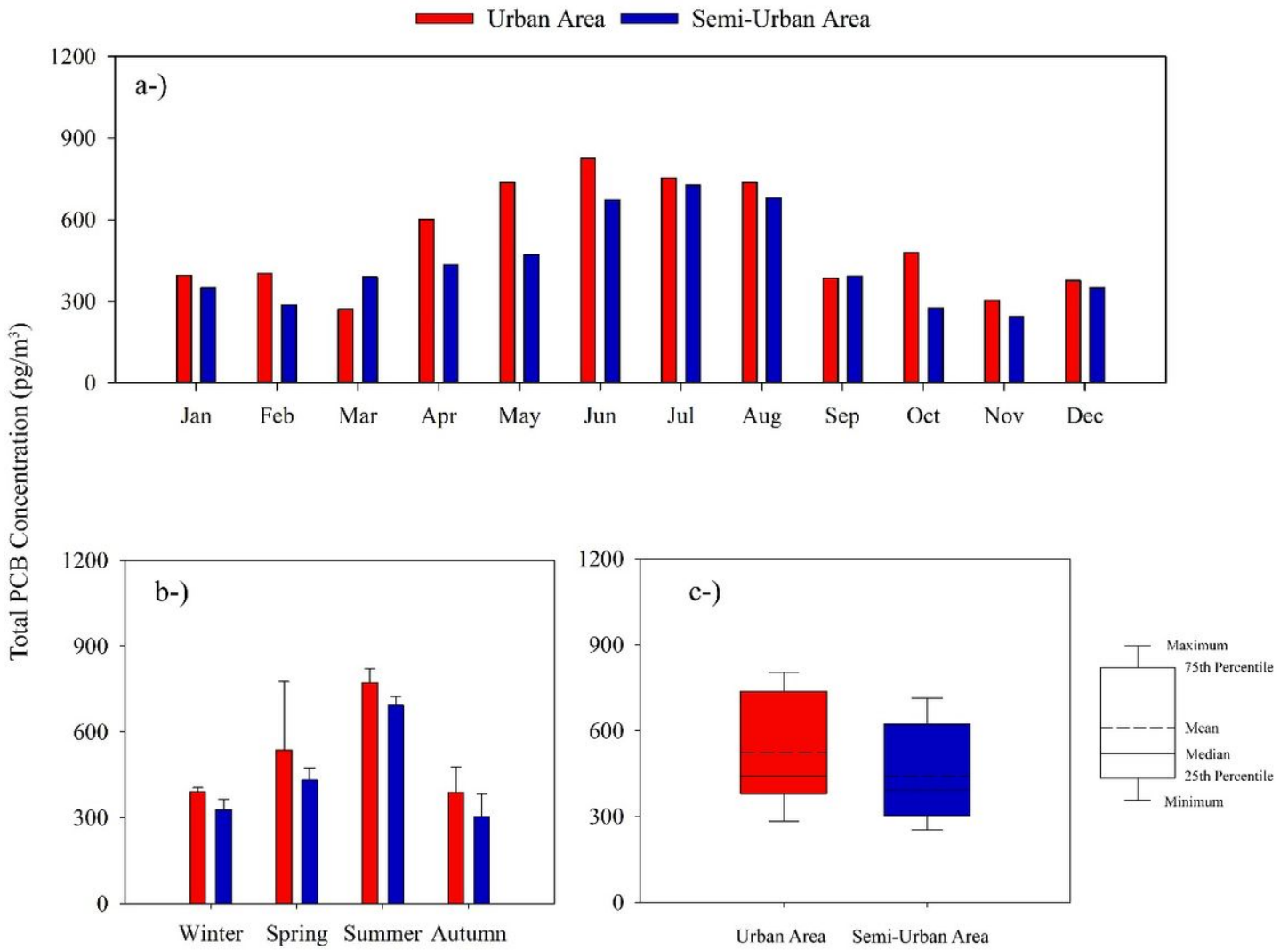


**Figure 3**

Monthly (a), seasonal (b) and annual (c) PCB distributions for the sampling areas

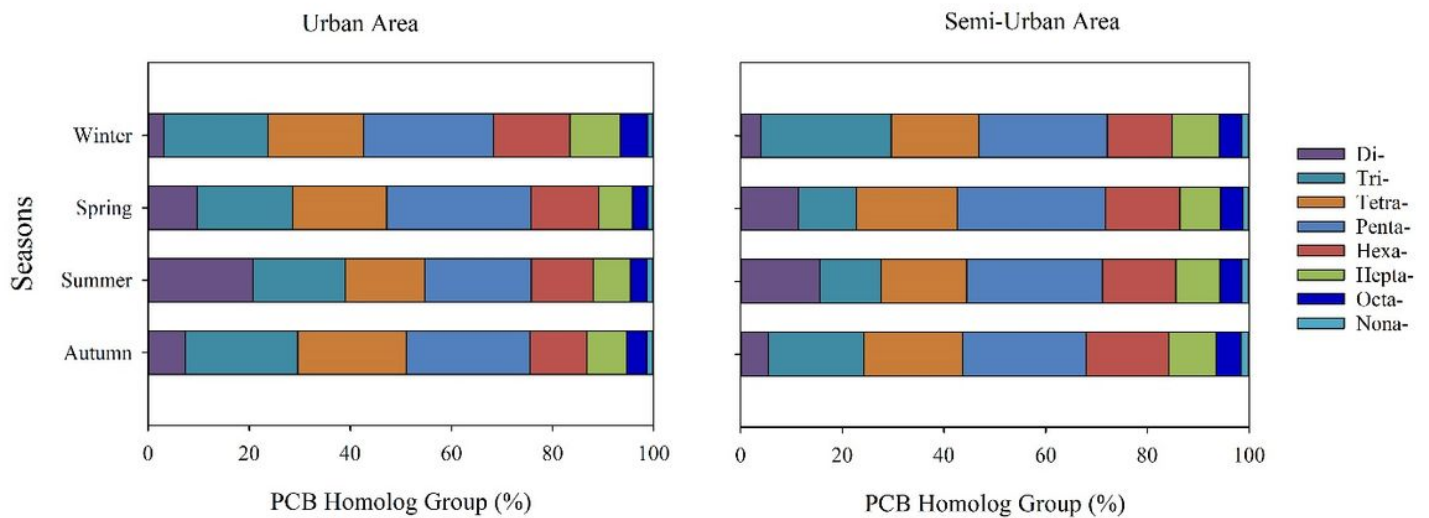


**Figure 4**

Seasonal homologous group distributions for urban and semi-urban areas

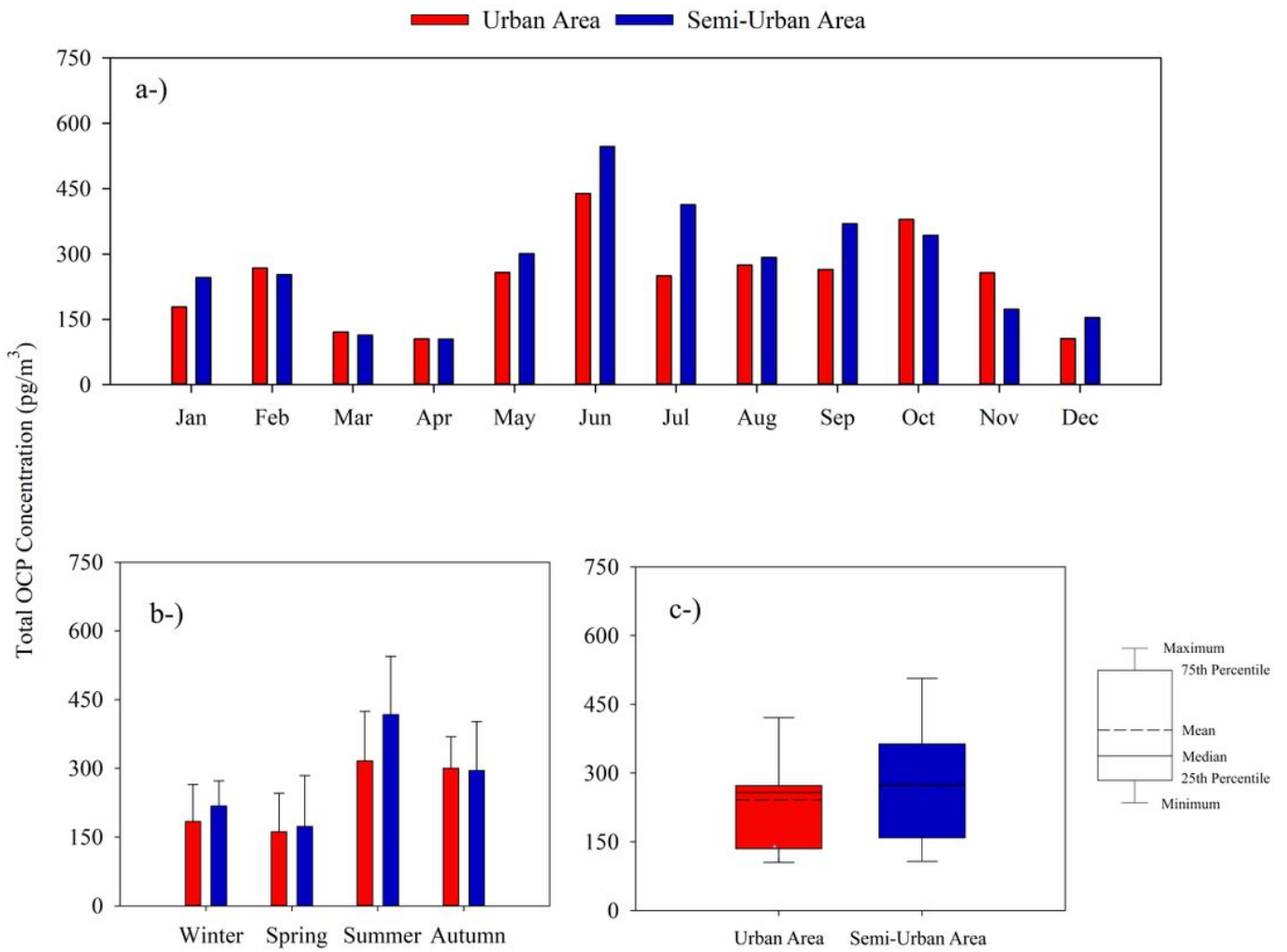


**Figure 5**

Monthly (a), seasonal (b) and annual (c) OCP distributions for the sampling areas

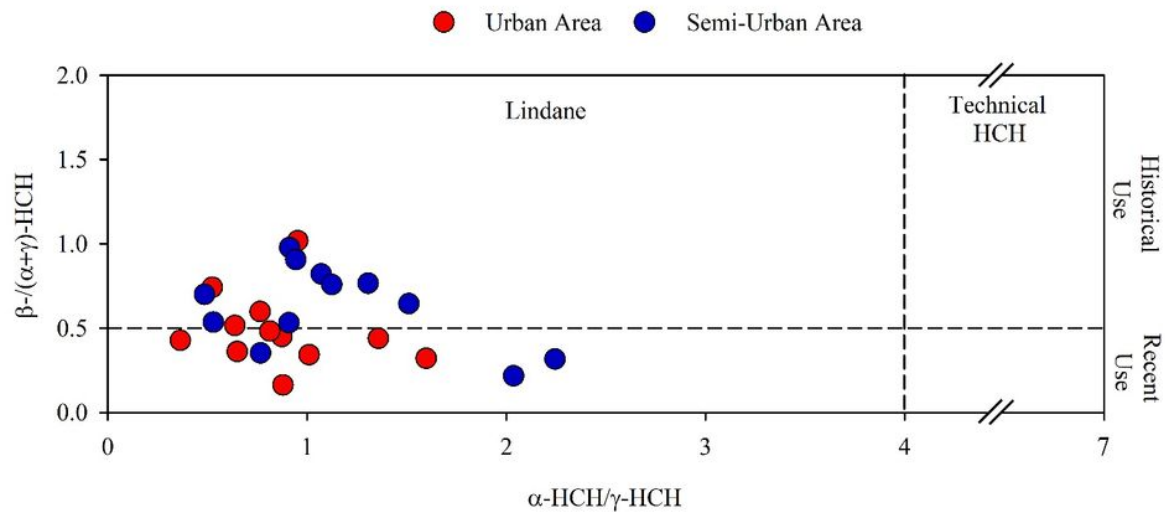


**Figure 6**

The ratio of  $\beta/(\alpha+\gamma)$ -HCH versus ( $\alpha$ -HCH /  $\gamma$ -HCH) for the urban and semi-urban areas

## Supplementary Files

This is a list of supplementary files associated with this preprint. Click to download.

- [SupplementaryMaterialsSariandEsen.docx](#)